Peer-reviewed version available at *Sensors* **2019**, *19*, 4249; doi:10.3390/s19194249

Article

Strategies for the Surface Modification with Ag Shaped Nanoparticles: Electrocatalytical Enhancement of Screen Printed Electrodes for the Detection of Heavy Metals

Karina Torres-Rivero[1,2]*, Lourdes Torralba-Cadena[1], Alexandra Espriu-Gascon[1,2], Ignasi Casas[1,2], Julio Bastos-Arrieta[3]*, Antonio Florido[1,2]

[1] Departament d'Enginyeria Química, Escola d'Enginyeria de Barcelona Est (EEBE), Universitat Politècnica de Catalunya, BarcelonaTEch (UPC), Av. Eduard Maristany 16, 08019 Barcelona, Spain; ltc_86@hotmail.com (L.T.-C.); alexandra.espriu@upc.edu (A.E.-G.); ignasi.casas@upc.edu (I.C.); antonio.florido@upc.edu (A.F.)

[2] Barcelona Research Center for Multiscale Science and Engineering, Av. Eduard Maristany 16, 08019 Barcelona, Spain

[3] Physical Chemistry TU Dresden, Zellescher Weg 19, 01069 Dresden, Germany

* Correspondence: julio.bastos@tu-dresden.de (J.B.-A.); karina.torres.rivero@upc.edu (K.T.-R.)

Abstract: The screen-printed carbon nanofibers electrodes (SPCNFE) represent an alternative with great acceptance due to their results, as well as their low impact for the environment. In order to improve their performance, in the present work they were modified with silver nanoparticles (Ag-NPs) and electrochemically characterized by using anodic stripping voltammetry. From the Ag-NPs synthesis, silver seeds (Ag-NS) and silver nanoprisms (Ag-NPr) were obtained. The Ag-NPs formation was confirmed by micrographs where Ag-NPs with diameters of 12.20±0.04 nm for Ag-NS, and 20.40±0.09 nm for Ag-NPr were observed. The electrodes were modified by using three different deposition methods: drop-casting, spin-coating and *in-situ* approaches. It was observed that the last methodology showed a low amount of Ag-NS deposited on the electrode surface and a deep alteration of this surface. Those facts suggested that the in situ synthesis methodology were not appropriate for the determination of heavy metals and it was discarded. The incorporation of the nanoparticles by spin-coating and drop-casting strategies showed different spatial distribution on the electrode surface as proved by scanning electron microscopy. The electrodes modified by these strategies, were evaluated for the cadmium(II) and lead(II) detection using differential pulse anodic stripping voltammetry, obtaining detection limit values of 2.1 and 2.8 μg L^{-1}, respectively. The overall results showed that the incorporation route does not change directly the electrocatalytic effect of the nanoparticles, but the shape of these nanoparticles (spherical for seeds and triangular for prisms) has a preferential electrocatalytical enhancement over Cd(II) or Pb(II).

Keywords: screen printed electrodes; Ag nanoparticles; drop-casting; spin-coating; nanoprisms; heavy metals; Differential pulse anodic stripping voltammetric; electrocatalysis

1. Introduction

In order to ensure water quality, World Health Organization (WHO) has published the maximum allowed concentration of pollutants in drinking water [1]. Among these pollutants, the concentration of heavy metal ions (HMI) is of special concern due to their toxicity and bioaccumulation.

As examples, As, Cr, Hg, Pb and Cd concentrations must be under 10, 50, 1, 10 and 3 μg·L^{-1}, respectively [1]. Such low values need to be determined by means of highly sensitive techniques like Flameless Atomic Adsorption Spectrophotometry (FAAS) [2], Inductively Coupled Plasma Optical

Peer-reviewed version available at Sensors 2019, 19, 4249; doi:10.3390/s19194249

Emission Spectroscopy (ICP-OES) [3] and Inductively Coupled Plasma Mass Spectrometry (ICP-MS) [4], among others, nevertheless require expensive equipment and specialized technicians. These facts increases both the analysis time and the operation costs.

In order to avoid those inconveniences, alternative methodologies can be used for the quantification of HMI as, for instance, electrochemical voltammetry. This technique offers, among other advantages, a low cost equipment, easy to handle, a relatively fast analysis, and it is suitable to be used as a portable quantification device [5–9]. Thus, regarding the determination of HMI, the improvement of the electrochemical performance and sensitivity to HMI are required.

Analysts have invested big efforts into the design of new electrochemical sensors by taking advantage of the electrocatalytic effect of nanomaterials. This is aimed by the incorporation of metallic nanoparticles (MNPs) [10], oxide nanoparticles (ONPs) or carbon nanoallotropes (as carbon nanotubes or graphene) in the electrode components. These nanomaterials reduce the electron transfer resistance at the electrode surface which leads to the decrease of the electron-transfer limited process and consequently the response of the electrode at low analyte concentration is catalyzed [11–13]. For example, it has been reported that with these modifications, the HMI concentration can be determined at values lower than 1 $\mu g \cdot L^{-1}$ which meets the WHO requirements for heavy metal quantification in drinking water samples.

More specifically, the incorporation of nanoparticles (NPs) on the sensor surface has shown good results for determination of As [14–16], Cr [17], Cu [10,18,19], Pb [10,18–20], Cd [5], Hg [7,21,22]. Most of these works used a screen printed electrode (SPE) modified with different types of NPs (Pt-NPs, Ag-NPs or Au-NPs) as electrocatalysts. The main advantages of using SPE are their versatility and the fact that they can be used as one-use disposable sensor (avoiding any possible carryover contamination from previous measurements). Additionally, they are cost efficient and easily tunable as well as suitable to be incorporated in portable devices.

There are different approaches to the modification of electrochemical sensors with nanomaterials. For instance, the modification used by Sanllorente-Méndez et al. [15] and Domínguez-Renedo et al. [17] was based on the electrochemical reduction of a $PtCl_6^{2-}$ solution by applying two different potentials (+0.5 V for 0.01 s and -0.7 V for 10 s) to prepare Pt-NPs directly on the SPE. The main disadvantages of these procedures are that the distribution of the NPs among the electrode surface cannot be controlled and agglomeration of NPs is very common, influencing directly the electrochemical response of the sensor.

On the other hand, Li et al. [7] carried out a dip coating strategy, by immersing the electrode into an Au-NPs colloidal solution overnight and then the authors dried the electrode at 80 ºC. A similar process was used by Pérez-Ràfols et al. [10], as they drop-casted Ag-NPs on the SPE surface, with a later drying stage of 30 min at 50ºC. In this case, the particle size distribution and morphology can be regulated by the NPs preparation, but there is still a lack control of the final distribution of the NPs on the modified surface.

Muñoz et al. [23] carried out the incorporation of NPs to carbon nanotubes/epoxy nanocomposite electrodes by physical and chemical approaches. These included the *in situ* modification of the transducer material (with control on NPs spatial distribution); the physical mixing of NPs into the electrode matrix and drop attachment (drop-casting) of a NPs containing solutions. The overall results showed an enhancement of the electrochemical response to hydrogen peroxide as analyte.

In this sense, the aim of this work is to evaluate the feasibility of different strategies to modify commercial screen-printed carbon nanofibers electrodes (SPCNFE) with shaped silver nanoparticles and therefore, compare the electrocatalytic effect of these NPs on the determination of Cd(II) and Pb(II) in water samples. More specifically, three procedures of Ag-NPs deposition are considered: drop-casting (DC), *in situ* (IS) and spin-coating (SC). Besides, the characterization of the NPs and the SPCNFE surface by means of electron microscopy is described. Finally, the electrochemical characterization by Differential Pulse Anodic Stripping Voltammetry (DPASV) of the modified sensors is also presented.

2. Materials and Methods

Peer-reviewed version available at Sensors 2019, 19, 4249; doi:10.3390/s19194249

2.1. Reagents and solutions

All chemicals were analytical grade and were used with no additional purification. Different reagents used for the Ag-NPs synthesis (sodium citrate, sodium polystyrene sulfonic acid (SPSS), and silver nitrate) were supplied by Sigma-Aldrich (Munich, Germany), sodium borohydride by Panreac (Barcelona, Spain) and ascorbic acid by Scharlab (Barcelona, Spain). Lead(II) nitrate and cadmium(II) nitrate were purchased from Fluka (Buchs, Switzerland) and VWR International LTD (Radnor, PA, USA), respectively. A 2072 μg L^{-1} of Pb(II) and a 1124 μg L^{-1} of Cd(II) solutions (corresponding to 10^{-5} mol L^{-1}) were prepared by sequential dilution from a 1000 mg L^{-1} stock solution. Metal solutions were standardized by ICP-AES, Perkin Elmer model Optima 3200 (Waltham, MA, USA) or by ICP-MS, Agilent model 7500cx (Santa Clara, CA, USA). A 0.1 mol L^{-1} acetate buffer solution (pH 4.5) prepared from acetic acid (Merck, Munich, Germany) and sodium acetate (Panreac, Barcelona, Spain) was used as electrolyte and for constant pH. All solutions were made with ultrapure water (18.2 MΩ·cm) obtained from a Milli-Q plus 185 system (Millipore, Burlington, MA, USA).

2.2. Electrodes

Commercial SPCNFE (Dropsens®, ref. 110CNF, Llanera, Spain) including working, counter and reference electrodes were used. The working electrode consisted on a disk of 4 mm diameter where the carbon nanofiber surface was modified with the silver nanoparticles (Ag-NPs-SPCNFE).

2.3. Nanoparticle Synthesis

Ag-nanoseeds (Ag-NS) and Ag-nanoprisms (Ag-NPr) were prepared as follows, based on the methodology described somewhere else [24,25].

Preparation of Ag-NS

Ag-NS were obtained by mixing under continuous stirring 5 mL of 2.5 mmol·L^{-1} sodium citrate, 0.25 mL of 500 mg·L^{-1} PSSS and 0.3 mL of 10 mmol· L^{-1} sodium borohydride. Afterwards, a solution of 0.5 mmol· L^{-1} silver nitrate was continuously added to the previous solution at 2 mL·min^{-1} rate by using a syringe pump from Kd Scientific, model KDS 510 (Holliston, MA, USA).

Preparation of Ag-NPr

Several aliquots in the range 400-1600 μL of the Ag-NS previously obtained were mixed with 5 mL of Milli-Q water and 75 μL of 10 mmol· L^{-1} ascorbic acid. Then, 3 ml of 0.5 mmol· L^{-1} silver nitrate were continuously added to each aliquot at 1 mL·min^{-1}. Finally, 0.5 mL of 25 mmol· L^{-1} sodium citrate was added to each solution in order to stabilize the obtained Ag-NPr.

2.4. Electrode Modification

Drop-casting methodology

The same methodology and conditions as previously studied by Pérez-Ràfols [10] were used in the modification of the SPCNFE by both Ag-NS and Ag-NPr. The deposition methodology consisted in placing 40 μL of the Ag-NPs aqueous solution on the working electrode surface of the SPCNFE and evaporate the solvent by heating it at 50ºC for 30 minutes. This procedure avoids damage to the Ag-NPs or electrical parts of the electrode and, at the same time, it ensures the removal of water.

Spin-coating methodology

Ag-NS and Ag-NPr were also used in the SPCNFE modification by the spin-coating methodology. A spin coater WS-650-8B from Laurell Technologies Corporation (North Wales, PA, USA) was used. The SPCNFE was attached to the center part of the spin coater by the vacuum system. Then, the different Ag-NPs were added onto the center part of the working electrode by placing 20 μL of the colloidal solution. The SPCNFE was then stirred under nitrogen atmosphere at 2000 rpm for 3 minutes inside the spin coater. A second 20 μL drop of Ag-NP was placed onto the same place and the same stirring methodology was performed again to the electrode.

In-situ Nanoparticle synthesis on electrode surface

Peer-reviewed version available at Sensors 2019, 19, 4249; doi:10.3390/s19194249

In this methodology a bare SPCNFE electrode was dipped in different beakers containing the following solutions: first it was immersed in a 3 mol·L^{-1} nitric acid for 1 h; afterwards in a 1 mol·L^{-1} sodium chloride; later in a 0.1 mol·L^{-1} silver nitrate and finally in a 0.2 mol·L^{-1} freshly prepared sodium borohydride, all of them for 30 minutes[23].

2.5. Characterization of the Ag-NPs and of the SPCNFE surface

UV/Vis Spectroscopy

The UV/Vis spectra showing the Surface Plasmon Resonance (SPR) of the Ag-NS and Ag-NPr colloidal solutions were recorded by using an Agilent-Hewlett Packard spectrophotometer, model 8453 (Waldbronn, Germany).

Electron Microscopy Characterization

Scanning Electron Microscopy (SEM)

Colloid solutions of Ag-NS and Ag-NPr nanoparticles were characterized by using a Gemini SEM from ZEISS® (Jena, Germany). Ag-NPs samples were prepared as in a previous work [26]. In addition, the surface of the SPCNFE electrodes was also studied by the SEM before and after the Ag-NPs deposition. This aimed to determine the NPs presence and their spatial distribution on the SPCNFE regarding the modification strategy: drop-casting, spin-coating or *in-situ*.

Transmission Electron Microscopy (TEM)

For further characterization of the Ag-NPs synthetized in this work, a JEM-2010 TEM from JOUL ® (Tokyo, Japan) was used. Ag-NPs samples were also conditioned as in a previous work [26]. From the TEM images, the size distribution of the obtained Ag-NPs was determined and the size distribution histograms were calculated as before [26] using the Image-J version 1.51m software.

2.6. Electrochemical Characterization of Ag-NPs-SPCNFE

Voltammetric studies of the SPCNFE modified electrodes were performed with a Multi Autolab/M204 - Modular Multi Potentiostat/Galvanostat and a personal computer with NOVA 2.1 software package to control the potentiostat as well as for the required data treatment, all from Metrohm (Herisau, Switzerland).

Cyclic voltammograms of bare and NPs modified electrodes were obtained in acetic acid/acetate buffer solution by scanning the potential from -1.00 to +1.00 V at a scan rate of 0.01 V·s^{-1} and a step potential of 0.00244 V.

Differential pulse anodic stripping voltammetric (DPASV) measurements by using Ag-NPs-SPCNFE for the determination of Pb(II) and Cd(II) ions were performed. A deposition potential (E_d) of -1.40 V applied under stirring conditions during a deposition time (t_d) of 180 of seconds and followed by a rest period (t_r) of 5 seconds were used. DPASV measurements were carried out under the following conditions: a scanning potential range from -1.40 to 0.00 V, a step potential of 5 mV, a pulse time of 50 ms and a pulse amplitude of 50 mV. All experiments were performed at room temperature (22 ± 1 °C) and without oxygen removal.

Measurements of Pb(II) and Cd(II) ions by DPASV were performed using bare electrodes and for each Ag-NPs-SPCNFE prepared by the different modification methodologies. Initially, the electrodes were calibrated for each HMI. For this purpose, increasing concentrations of Pb(II) and Cd(II) solutions were added to an initial 40 mL of acetic/acetate buffer solution. Calibration samples ranged from 1.0 to 100.0 and from 1.0 to 75.0 µg L^{-1} for Pb(II) and Cd(II), respectively.

3. Results and Discussion

3.1. UV/Vis Spectroscopy Characterization

The formation of the Ag-nanoparticles, perceived by simple visual observation of the color, was monitored by the UV-Vis spectra of the different colloidal solutions. Thus, to the initial Ag-NS

Peer-reviewed version available at Sensors 2019, 19, 4249; doi:10.3390/s19194249

suspension, different volumes ranging between 400 and 1600 µL of the Ag-NS colloidal solution were added. Figure 1 shows the spectra obtained for the Ag-NS and for Ag-NPr synthesized by using the different volumes of Ag-seed solution already mentioned. It can be observed that the Ag-NPr nanoparticles with less amount of seed solution (400 µL) showed an absorbance peak at 570 nm further away from to the initial seeds' absorbance peak at 405 nm. However, colloidal solutions with higher amounts of the added Ag-NS solution presented absorbance bands that shifted to lower wavelengths getting closer to the original Ag-NS solution (see Figure 1). The obtained wavelengths agreed with previously reported values where silver colloids exhibit maximum absorbance within the range 400–500 nm due to Surface Plasmon Resonance (SPR) [27–29]. It must be mentioned that the peak absorbance of the 400 µL Ag-NS solution was higher than all the others and when higher volumes of Ag-NS solution were added, peaks heights decreased to values getting closer to the ones presented by the initial Ag-NS solution. Moreover, the shift (from 405 nm in the initial Ag-NS solution) towards larger wavelengths (570 nm in 400 µL solution) could also indicate an increase in the mean diameter of Ag-nanoparticles [30,31]. For all this, the Ag-NS and the Ag-NPr obtained from a volume of 400 µL of Ag-NS solution were used in the next studies.

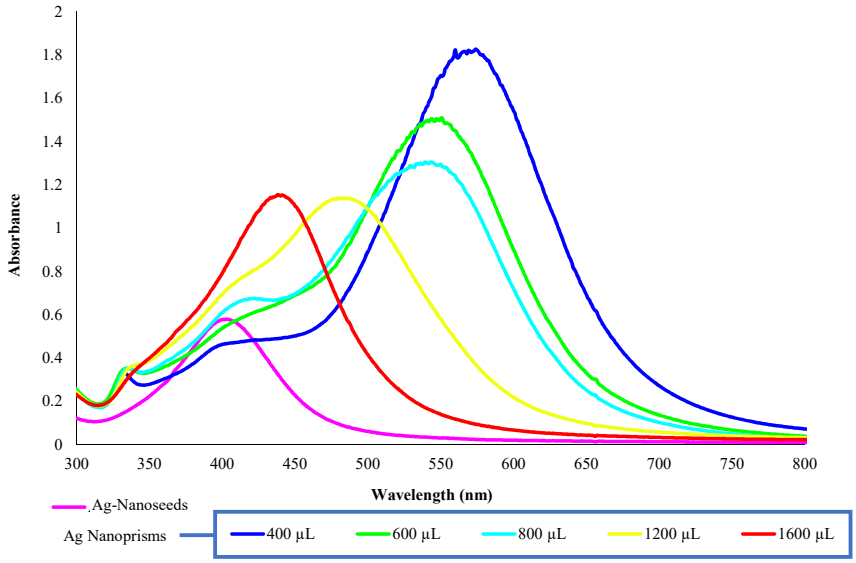

Figure 1. UV/Vis spectra obtained for the Ag-nanoseeds and for Ag-nanoprisms synthesized by using different volumes of Ag-seed solution: 400, 600, 800, 1200 and 1600 µL.

3.2. Electron Microscopy Characterization

3.2.1. Characterization of Ag-nanoparticles by TEM and SEM

Figure 2 shows the electron microscopy characterization of the studied Ag-NPs samples. The SEM image of the Ag-NS can be observed in Figure 2a (white dots), confirming the effectivity of the synthesis procedure followed. Additionally, Figure 2c shows the size distribution histogram obtained from a total of 400 Ag-NS. The nanoparticle counting was performed following the same procedure and using the same software as reported previously [26]. These results show that the Ag-NS obtained present an average diameter of 12.2 ± 0.4 nm.

Peer-reviewed version available at Sensors 2019, 19, 4249; doi:10.3390/s19194249

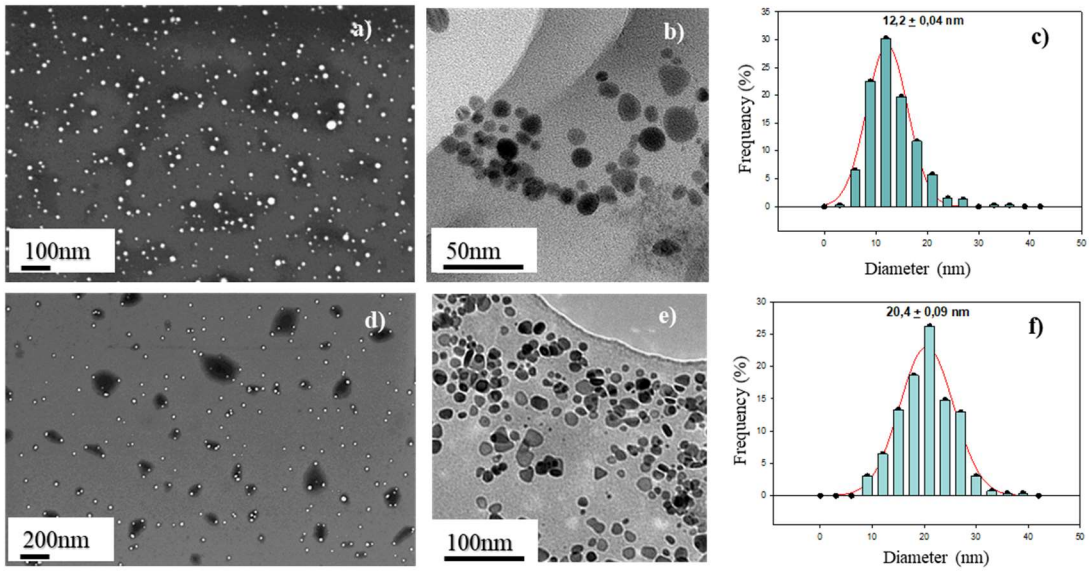

Figure 2. Characterization of the Ag-nanoseeds (a, b, c) and Ag-nanoprisms (d, e, f). SEM images (a, d); TEM images (b, e) and Size Distribution Histograms (c, f), respectively.

From the TEM image presented in Figure 2b it can be deduced that most of Ag-NS present a spherical shape. These structures are in good agreement with reported shapes of Ag-NPs [24,25].

The SEM resulting image of the Ag-NPr obtained can be observed as white dots in Figure 2d. The diameter distribution histogram of the Ag-NPr (see Figure 2f) show that the average particle size was 20.4 ± 0.09 nm. Compared with the Ag-NS, Ag-NPr are bigger and present a slight wider size distribution than the Ag-NS. These results confirmed the transformation of Ag-NS to Ag-NPr as described previously [24,25]

3.2.2. Electrode Characterization by SEM

In Figure 3, the SEM InLens images of the different electrodes obtained as explained above is presented in order to compare the final surface obtained. The Ag-NS were located into the carbon fibers, identified as circled white spots in the images of the Figures 3 b, c and d.

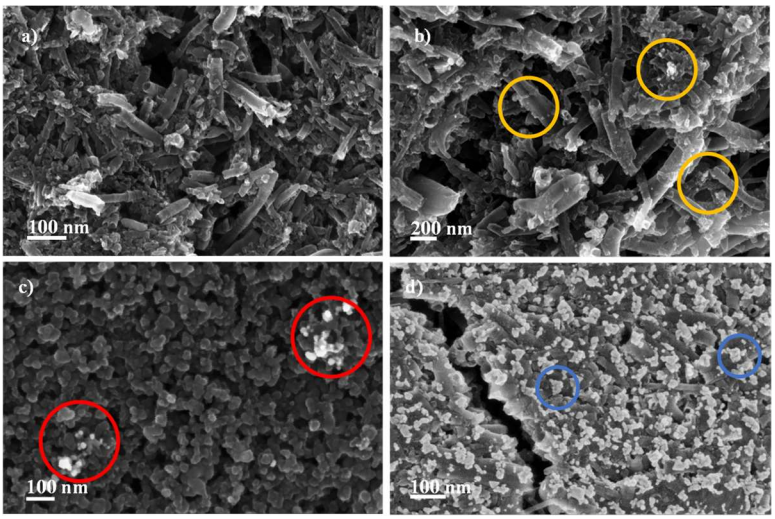

Figure 3. SEM InLens images of the electrodes used in this work. a) Bare commercial SPCNFE; b) Ag-NS-SPCNFE modified by drop-casting method; c) Ag-NS-SPCNFE modified by *in-situ* synthetic method; d) Ag-NS-SPCNFE modified by spin-coating method. Examples of Ag-nanoparticle location is indicated with colored circles.

Figure 3c shows the Ag-NPs incorporation by the *in situ* methodology. It can be observed that the modification of the electrode surface was not acceptable due the low amount of Ag-NS deposited.

Peer-reviewed version available at Sensors 2019, 19, 4249; doi:10.3390/s19194249

In addition, the mechanical resistance of the SPCNFE was compromised as some changes on the substrate were observed (change of color of the electrode connectors) that could be caused by the $NaBH_4$. Additionally, blank electrodes were prepared by the IS approach and their response signal was lost in all cases, showing that this modification strategy was not appropriate to functionalize the electrode surface with NPs. Therefore, the IS strategy was not used for the determination of heavy metals.

The SEM images of the electrodes prepared by drop-casting of Ag-NS (Figure 3b), indicated in this case a successful modification of the electrode, with Ag-NS visible over the electrode surface. Finally, the electrodes prepared by the spin-coating approach showed a strong modification of the SPCNFE electrode (Figure 3d) with a larger amount of deposited Ag-NPs as compared with the two previous methodologies. This effect could be attributed to a better and uniform dispersion of the nanoparticle suspension over the electrode substrate, due to the speed of the spray coating process itself. Based on the characterizations performed, it was decided to continue the work only using the two electrodes with successful incorporation of the NPs to the electrode surface.

3.3. Electrochemical characterization of the electrodes

3.3.1. Preliminary Studies of the SPCNFE modification with Ag-nanoparticles

In order to determine if the modification of SPCNFE with Ag-nanoparticles resulted in the enhancement of their electrochemical response, Cyclic Voltammetry (CV) and Differential Pulse Anodic Stripping Voltammetry (DPASV) were performed.

First, the cyclic voltammograms of both the bare and the Ag-NPs modified electrodes were carried out, as seen in Figure 4. It can be seen that the current intensity of the oxidation peaks at 0.2 V (Ag-NPs) of the Ag-NS-SPCNFE and Ag-NPr-SPCNFE are very similar, suggesting that the Ag-NPs concentration on the WE surface would be comparable, which is important for the evaluation of both strategies.

It seems that SC strategy offers a more consistent approach in terms of amount of NPs incorporated to the SPCNFE. DC strategy depends on factors like solvent evaporation and appropriate location of the drop, this can explain the different signal obtained regarding the amount of NPs incorporated, although for the case of DC- Ag-NPr, the signals agree accordingly to the SC strategy.

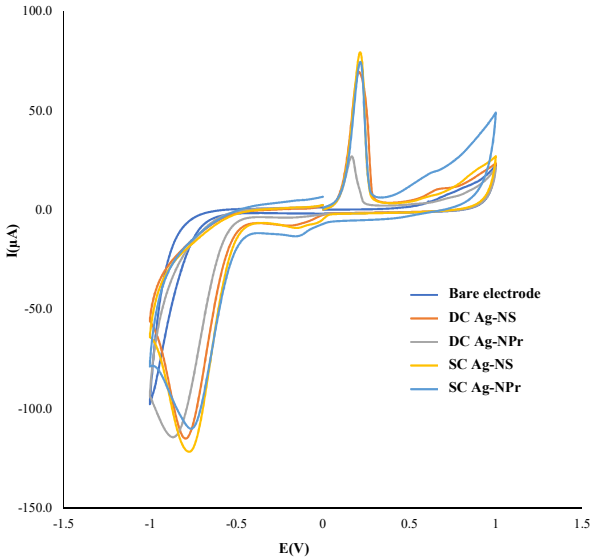

Figure 4: Cyclic voltammograms in acetic acid/acetate buffer at pH 4.5 of Ag-nanoseeds and Ag-nanoprisms based SPCNFE electrodes obtained by using either drop-casting (DC) or spin-coating (SC) methodologies.

As seen in Figure 4, current peaks obtained in the case of Ag-NS-SPCNFE were higher than in the case of Ag-NPr-SPCNFE. Even though this effect might be caused by the fact that the amount of

Peer-reviewed version available at Sensors 2019, 19, 4249; doi:10.3390/s19194249

Ag-NPs on both electrode surface could be different due to the different Ag-NPs concentration on the colloidal solutions, another reason could be related to the specific surface area of the Ag-NPs. As it was shown in Figure 2, smaller nanoparticles were obtained in the case of Ag-NS than in Ag-NPr and this would probably result in a better response of the Ag-NS-SPCNFE

In order to study the electrochemical response comparing a bare SPCNFE electrode and a Ag-NPs-SPCNFE in the determination of Pb(II) or Cd(II), differential pulse anodic stripping voltammetry (DPASV) measurements were performed in solutions containing either 70.0 μg L^{-1} of Pb(II) or Cd(II). From the results obtained (see Figure 5), it can be concluded that the modification of the electrodes by Ag-NPs caused a significant increase in the electrode response and would be an interesting alternative in the determination of both metal ions.

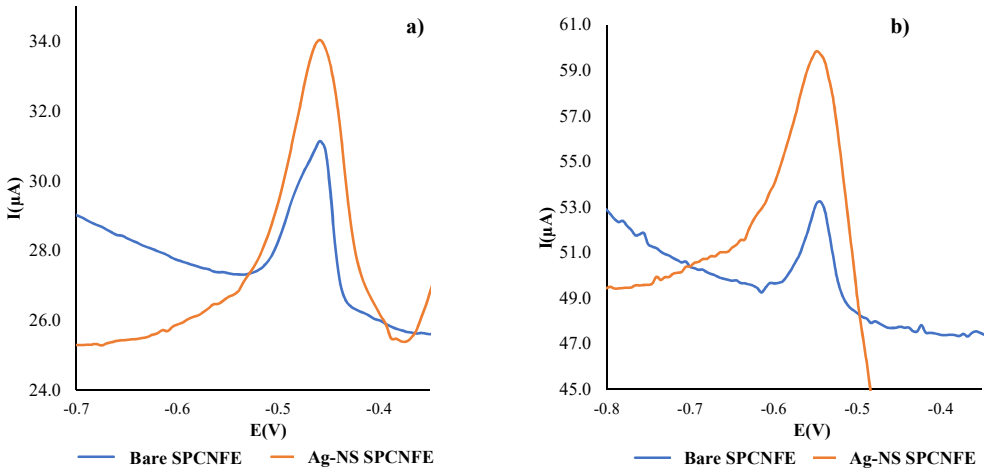

Figure 5. Differential pulse anodic stripping voltammetry (DPASV) measurements of non-modified SPCNFE and Ag-nanoseeds-SPCNFE electrodes obtained for a 70 μg·L-1 of a) lead(II) or b) cadmium(II) ions. Experimental conditions: acetic acid/acetate buffer pH 4.5 with an Ed of -1.40 V applied during a td of 180 seconds and employing a step potential of 5 mV, a pulse time of 50 ms and a pulse amplitude of 50 mV.

3.3.2. Study of Ag-NS-SPCNFE electrodes obtained by either drop-casting (DC) or spin-coating (SC) methodologies

Single calibration curves by DPASV were performed by increasing the concentration of Pb(II) and Cd(II) in the range from 1.0 to 100.0 and from 1.0 to 75.0 μg L^{-1}, respectively. The same procedure was followed for either DC or SC electrodes. From the data obtained, detection limits were determined by using the Miller & Miller procedure [32,33].

Results of the calibration parameters as detection limits (LOD), linear ranges and linearity are listed in Table I. The limit of quantification (LOQ) is considered as the lower value of the linear range. As an example, the voltammogram related to the Pb(II) response and the corresponding calibration plot of Ag-NS-SPCNFE for DC and SC deposition methods are shown in Figure 6.

Peer-reviewed version available at Sensors 2019, 19, 4249; doi:10.3390/s19194249

Table I. Calibration parameters as limits of detection (LOD), linear ranges and linearity obtained for the determination of Pb(II) and Cd(II) on Ag-nanoseeds-SPCNFE and Ag-nanoprisms-SPCNFE and for drop-casting (DC) and spin-coating (SC) methodologies.

	Pb(II)			Cd(II)		
Deposition/Ag-NPs	**LOD (µg·L^{-1})**	**Linear Range (µg·L^{-1})**	**R^2**	**LOD (µg·L^{-1})**	**Linear Range (µg·L^{-1})**	**R^2**
DC Ag-nanoseeds	3.3	10.9-99.6	0.9990	3.7	12.2-73.4	0.9923
SC Ag-nanoseeds	2.8	9.4-99.6	0.9990	2.4	8.1-73.4	0.9976
DC Ag-nanoprisms	3.1	10.3-18.3	0.9840	2.2	7.4-73.4	0.9980
SC Ag-nanoprisms	3.4	11.3-50.3	0.9911	2.1	6.9-73.4	0.9976

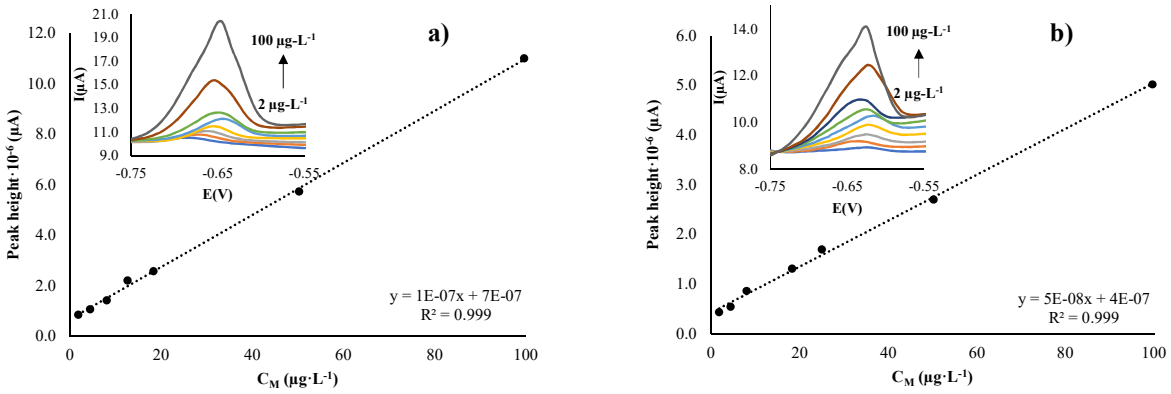

Figure 6. Calibration curves and DPASV measurements (insets) for Pb(II) calibration obtained with the Ag-nanoseeds-SPCNFE electrodes using a) drop-casting and b) spin-coating methodologies. Same experimental conditions as in Figure 4.

It can be seen from the DPASV curves presented in Figure 6 that a stable oxidizing peak appears around -0.64 V, which corresponds with the increasing concentration of Pb(II) in both approaches. Comparing the results obtained with Ag-NS with the ones obtained with the bare electrode, it can be concluded that the electrode electrocatalytic response is clearly enhanced. This result agrees with previous reported works that stated the effect of Ag-NPs on the increased sensitivity and analytical features of the modified SPCNFE [10,26].

Table I shows that in all cases, electrodes presented good and similar performance in terms of LOD with slightly better values in the case of the spin-coating method. In terms of metal ions response, it can be observed that Ag-NS electrodes showed better linear regressions and wider linear ranges in the Pb(II) calibrations than in the Cd(II) response. This behavior was obtained for both modification strategies, and it seems that the electrocatalytic enhancement relays only on the presence of the NPs but it does not seem to be associated to the incorporation route. As it was seen in SEM images, in SC deposition most of the NPs are homogenously distributed on the surface of the electrode (externally localized), while for DC, it seems that there is some diffusion into the matrix (internally localized). SC is a common technique used to produce uniform thin films (e.g. of organic materials) with customized thicknesses of the order of micrometers and nanometers. For the case of the preparation of NPs films, the coating depends on the NPs concentration. One crucial parameter to control in SC is the spin acceleration, which drives the fluid thinning, solvent evaporation and consequently, the film formation [34]. On the other hand, the DC deposition depends on the evaporation rate due to the temperature and the uniform coating during the casting. It seems that

Peer-reviewed version available at Sensors 2019, 19, 4249; doi:10.3390/s19194249

interaction between the casting and evaporation in DC leads to the NPs penetration into the nanofiber matrix.

In all cases, the LODs values obtained for both deposition methods are close to 3 μg L^{-1}. It is important to point out that these values are below or at least at the same order of magnitude of the legislated values in the case of Pb(II) and Cd(II) concentrations in drinking waters [1].

3.3.3. Study of Ag-NPr-SPCNFE electrodes prepared by either drop-casting (DC) or spin-coating (SC) methodologies

By following a similar procedure as before, Ag-NPr electrodes were studied and their response to Pb(II) and Cd(II) concentrations was determined. Results of the calibration parameters are presented in Table I. From this data, it can be determined that slightly better electrochemical performance was observed in the case of Cd(II) response for this kind of Ag-NPs. In Figure 7 it can be observed a stable and measurable signal when Cd(II) concentration is increased. This performance was seen in both DC and SC methodologies, and the current signal improved in a relevant way compared with the bare electrode.

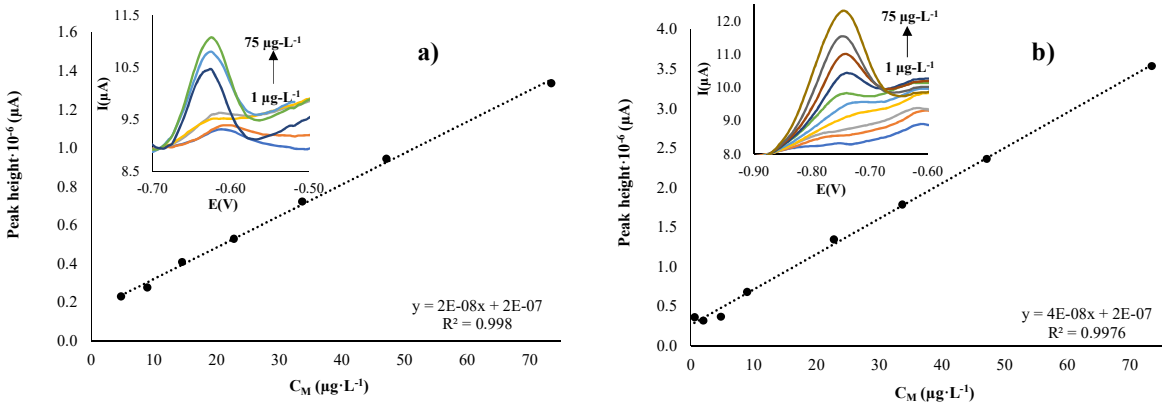

Figure 7. Calibration curves and DPASV measurements (insets) for Cd(II) calibration obtained with the Ag-nanoprisms-SPCNFE electrodes using a) drop-casting and b) spin-coating methodologies. Same experimental conditions as in Figure 4.

From the data presented in Table I, it can be pointed out that Ag-NPr electrodes presented slightly better LOD values, better linear regressions and wider linear ranges in the Cd(II) calibrations than in the Pb(II) response. However, non-significant differences were seen in this case in terms of drop-casting or spin-coating methodologies. This would confirm the results mentioned for Ag-NS-SPCNFE that the modification methodology would not be a determinant factor in the enhancement of the response of the electrodes.

Additionally, as it was already mentioned, LODs obtained for Ag-NPr-SPCNFE in both deposition methods and for both studied ions were around 3 μg L^{-1}. These values are also below the legislated values for the determination of Pb(II) and Cd(II) concentration in drinking waters. Nevertheless, a comparison among all the response characteristics for both Ag-NPs studied could conclude that Ag-NS would be more suitable in the determination of Pb(II), meanwhile Ag-NPr would result more appropriate to determine Cd(II). This can be mainly attributed to the different reactivity that these NPs can have due to their shape.

Peer-reviewed version available at Sensors 2019, 19, 4249; doi:10.3390/s19194249

4. Conclusions

In this work, three different deposition methodologies: *in situ*, drop-casting and spin-coating, have been evaluated as feasible strategies for the modification of screen-printed carbon nanofibers electrodes (SPCNFE) with two different shaped nanoparticles: Ag-NS and Ag-NPr. For this, the formation of each type of Ag-NPs was monitored by UV-Vis. Moreover, electron microscopy was used in the characterization of their size, shape and distribution on the SPCNFE surface. The obtained Ag-NS presented an average diameter of 12.2 ± 0.04 nm and, in general, showed a spherical shape. On the other hand, in the case of Ag-NPr, the obtained average particle size was 20.4 ± 0.09 nm and, among a variety of shapes, mostly showed a triangular shape. The electrode modification approaches were studied by Scanning Electron Microscopy. In two of them, drop-casting and spin-coating, SEM images indicated a correct modification of the electrode, with Ag-NPs embedded inside or all over the carbon nanofibers. Additionally, in the case of the spin-coating methodology, SEM images showed a strong modification of the SPCNFE with many and more uniformed Ag-nanoparticles deposited due to the high speed of the spin coater. Finally, the *in situ* methodology showed a low amount of Ag-NS deposited on the electrode surface and a deep alteration of this surface. Those facts suggested that the *in situ* synthesis methodology were not appropriate for the electrode modification and it was discarded.

Finally, electrochemical characterizations of the Ag-NPs-SPCNFE and their application in the determination of Pb(II) and Cd(II) ions were carried out. The results obtained in the case of Ag-NS and Ag-NPr based SPCNFE electrodes for both studied metal ions and for the DC and SC deposition strategies indicated appropriate and similar performances in terms of LOD with values around 3 μg L^{-1}. In terms of metal ions response, it was observed that Ag-NS electrodes showed better linear regressions and wider linear ranges in the case of Pb(II) calibrations, meanwhile for Ag-NPr electrodes better results were obtained for Cd(II) response. This behavior was obtained for both DC and SC methodologies. A comparison among all the response characteristics for both Ag-NPs studied could conclude that Ag-NS would be more suitable in the determination of Pb(II), while Ag-NPr would result more appropriate to determine Cd(II). On the other hand, an evaluation of the effect of the modification methodology on the Ag-NPs-SPCNFE response indicated that using DC or SC deposition methods seemed not to be a parameter that enhanced the response of the SPCNFE electrodes, even though better Ag-NPs distribution was observed by SEM images in the case of SC methodology. Therefore, it can be concluded that the spatial distribution of the NPs in the SPCNFE does not play a significant effect on the detection, under the conditions of the present study. However, their presence is the one giving the electrocatalytic enhancement, so the electrode substrate acts as the only component during the electrochemical detection. Nevertheless, SC approach can be considered more time and cost efficient, which makes it a more environmentally friendly approach for the modification of electrodes.

Additionally, LODs obtained in both deposition methods, Ag-NPs and for both studied ions (around 3 μg L^{-1}) are below or at least the same order of the legislated values in the case of Pb(II) and Cd(II) concentration in drinking waters. For all this, Ag-NPs-SPCNFE could be an accurate, portable and sensible analytical system for the determination of Pb(II) or Cd(II) in natural waters.

Author Contributions: K.T.-R. and L.T.-C. had contributed exactly the same and both are first authors. Conceptualization, A.F. and J.B.-A.; Methodology, A.F., J.B.-A. and A.E.-G.; Investigation, L.T.-C. and K.T.-R.; Validation, A.F., J.B.-A., A.E.-G., L.T.-C. and K.T.-R.; Formal Analysis, A.F., I.C., J.B.-A., A.E.-G., L.T.-C. and K.T.-R.; Resources, A.F. and I.C.; Writing-Original Draft Preparation, L.T.-C., A.E.-G. and K.T.-R.; Writing-Review & Editing, A.F., J.B.-A. and I.C.; Supervision, A.F., I.C. and J.B.-A.; Project Administration, A.F.; Funding Acquisition, A.F

Funding: This research has been funded by Ministerio de Ciencia, Innovación y Universidades and European Union Funds for Regional Development (FEDER), projects CTM2015-68859-C2-2-R and ENE2017-83048-R, and by the Generalitat de Catalunya (Project 2017SGR312.

Acknowledgments: Lourdes Torralba-Cadena also acknowledges the Consejo Nacional de Ciencia y Tecnología (CONACyT), United Mexican States for a Master grant.

Peer-reviewed version available at Sensors 2019, 19, 4249; doi:10.3390/s19194249

Conflicts of Interest: The authors declare no conflict of interest.

References

1. Edition, F. Guidelines for drinking-water quality. *WHO Chron.* **2011**, *38*, 104–108.
2. Daşbaşi, T.; Saçmaci, Ş.; Çankaya, N.; Soykan, C. A new synthesis, characterization and application chelating resin for determination of some trace metals in honey samples by FAAS. *Food Chem.* **2016**, *203*, 283–291.
3. Massadeh, A.M.; Alomary, A.A.; Mir, S.; Momani, F.A.; Haddad, H.I.; Hadad, Y.A. Analysis of Zn, Cd, As, Cu, Pb, and Fe in snails as bioindicators and soil samples near traffic road by ICP-OES. *Environ. Sci. Pollut. Res.* **2016**, *23*, 13424–13431.
4. Miao, L.; Ma, Y.; Xu, R.; Yan, W. Geochemistry and genotoxicity of the heavy metals in mine-abandoned areas and wasteland in the Hetai goldfields, Guangdong Province, China. *Environ. Earth Sci.* **2012**, *65*, 1955–1964.
5. Lei Zhang; Da-Wei Li; Wei Song; Lei Shi; Yang Li; Yi-Tao Long High Sensitive On-Site Cadmium Sensor Based on AuNPs Amalgam Modified Screen-Printed Carbon Electrodes. *IEEE Sens. J.* **2010**, *10*, 1583–1588.
6. Zhang, X.; Zhang, Y.; Ding, D.; Zhao, J.; Liu, J.; Yang, W.; Qu, K. On-site determination of Pb2+and Cd2+in seawater by double stripping voltammetry with bismuth-modified working electrodes. *Microchem. J.* **2016**, *126*, 280–286.
7. Li, D.; Li, J.; Jia, X.; Wang, E. Gold nanoparticles decorated carbon fiber mat as a novel sensing platform for sensitive detection of Hg(II). *Electrochem. commun.* **2014**, *42*, 30–33.
8. El-Mai, H.; Espada-Bellido, E.; Stitou, M.; García-Vargas, M.; Galindo-Riaño, M.D. Determination of ultra-trace amounts of silver in water by differential pulse anodic stripping voltammetry using a new modified carbon paste electrode. *Talanta* **2016**, *151*, 14–22.
9. Frutos-Puerto, S.; Miró, C.; Pinilla-Gil, E. Nafion-Protected Sputtered-Bismuth Screen-Printed Electrode for On-site Voltammetric Measurements of Cd(II) and Pb(II) in Natural Water Samples. *Sensors* **2019**, *19*, 279.
10. Pérez-Ràfols, C.; Bastos-Arrieta, J.; Serrano, N.; Díaz-Cruz, J.; Ariño, C.; de Pablo, J.; Esteban, M. Ag Nanoparticles Drop-Casting Modification of Screen-Printed Electrodes for the Simultaneous Voltammetric Determination of Cu(II) and Pb(II). *Sensors* **2017**, *17*, 1458.
11. Guo, Z.; Li, D.; Luo, X.; Li, Y.; Zhao, Q.-N.; Li, M.; Zhao, Y.; Sun, T.; Ma, C. Simultaneous determination of trace Cd(II), Pb(II) and Cu(II) by differential pulse anodic stripping voltammetry using a reduced graphene oxide-chitosan/poly-l-lysine nanocomposite modified glassy carbon electrode. *J. Colloid Interface Sci.* **2017**, *490*, 11–22.
12. Priya, T.; Dhanalakshmi, N.; Thennarasu, S.; Thinakaran, N. A novel voltammetric sensor for the simultaneous detection of Cd2+and Pb2+using graphene oxide/κ-carrageenan/L-cysteine nanocomposite. *Carbohydr. Polym.* **2018**, *182*, 199–206.
13. Li, J.; Guo, S.; Zhai, Y.; Wang, E. High-sensitivity determination of lead and cadmium based on the Nafion-graphene composite film. *Anal. Chim. Acta* **2009**, *649*, 196–201.
14. Idris, A.O.; Mabuba, N.; Arotiba, O.A. Electrochemical co-detection of Arsenic and Selenium on a Glassy Carbon Electrode Modified with Gold Nanoparticles. *Int. J. Electrochem. Sci.* **2017**, *12*, 10–21.
15. Sanllorente-Méndez, S.; Domínguez-Renedo, O.; Arcos-Martínez, M.J. Determination of arsenic(III) using platinum nanoparticle-modified screen-printed carbon-based electrodes. *Electroanalysis* **2009**, *21*, 635–639.
16. Cinti, S.; Politi, S.; Moscone, D.; Palleschi, G.; Arduini, F. Stripping Analysis of As(III) by means of screen-printed electrodes modified with gold nanoparticles and carbon black nanocomposite. *Electroanalysis* **2014**, *26*, 931–939.
17. Domínguez-Renedo, O.; Ruiz-Espelt, L.; García-Astorgano, N.; Arcos-Martínez, M.J. Electrochemical determination of chromium(VI) using metallic nanoparticle-modified carbon screen-printed electrodes. *Talanta* **2008**, *76*, 854–858.
18. Wan, H.; Sun, Q.; Li, H.; Sun, F.; Hu, N.; Wang, P. Screen-printed gold electrode with gold nanoparticles modification for simultaneous electrochemical determination of lead and copper. *Sensors Actuators, B Chem.* **2015**, *209*, 336–342.
19. Xiong, W.; Zhou, L.; Liu, S. Development of gold-doped carbon foams as a sensitive electrochemical sensor for simultaneous determination of Pb (II) and Cu (II). *Chem. Eng. J.* **2016**, *284*, 650–656.
20. Sivasubramanian, R.; Sangaranarayanan, M. V. Detection of lead ions in picomolar concentration range using underpotential deposition on silver nanoparticles-deposited glassy carbon electrodes. *Talanta* **2011**, *85*, 2142–2147.
21. Bui, M.P.N.; Brockgreitens, J.; Ahmed, S.; Abbas, A. Dual detection of nitrate and mercury in water using disposable electrochemical sensors. *Biosens. Bioelectron.* **2016**, *85*, 280–286.
22. Ratner, N.; Mandler, D. Electrochemical detection of low concentrations of mercury in water using gold

Peer-reviewed version available at Sensors 2019, 19, 4249; doi:10.3390/s19194249

nanoparticles. *Anal. Chem.* **2015**, *87*, 5148–5155.
23. Munoz, J.; Bastos-Arrieta, J.; Munoz, M.; Muraviev, D.; Céspedes, F.; Baeza, M. Simple green routes for the customized preparation of sensitive carbon nanotubes/epoxy nanocomposite electrodes with functional metal nanoparticles. *RSC Adv.* **2014**, *4*, 44517–44524.
24. Aherne, D.; Ledwith, D.M.; Gara, M.; Kelly, J.M. Optical properties and growth aspects of silver nanoprisms produced by a highly reproducible and rapid synthesis at room temperature. *Adv. Funct. Mater.* **2008**, *18*, 2005–2016.
25. Aherne, D.; Cara, M.; Kelly, J.M.; Gun'Ko, Y.K. From Ag nanoprisms to triangular AuAg nanoboxes. *Adv. Funct. Mater.* **2010**, *20*, 1329–1338.
26. Bastos-Arrieta, J.; Florido, A.; Pérez-Ràfols, C.; Serrano, N.; Fiol, N.; Poch, J.; Villaescusa, I. Green Synthesis of Ag Nanoparticles Using Grape Stalk Waste Extract for the Modification of Screen-Printed Electrodes. *Nanomaterials* **2018**, *8*, 946.
27. Fran ccedil ois, E. rsquo ane M.; Marcelle, L.S.; Cecile, O.E.; Agnes, A.N.; Djiopang, Y.S.; Fanny, A.E.M.; Lidwine, N.; Harouna, M.; Emmanuel, M.M. Unexplored vegetal green synthesis of silver nanoparticles: A preliminary study with Corchorus olitorus Linn and Ipomea batatas (L.) Lam. *African J. Biotechnol.* **2016**, *15*, 341–349.
28. Demirbas, A.; Welt, B.A.; Ocsoy, I. Biosynthesis of red cabbage extract directed Ag NPs and their effect on the loss of antioxidant activity. *Mater. Lett.* **2016**, *179*, 20–23.
29. Velgosová, O.; Mražíková, A.; Marcinčáková, R. Influence of pH on green synthesis of Ag nanoparticles. *Mater. Lett.* **2016**, *180*, 336–339.
30. Khalil, M.M.H.; Ismail, E.H.; El-Baghdady, K.Z.; Mohamed, D. Green synthesis of silver nanoparticles using olive leaf extract and its antibacterial activity. *Arab. J. Chem.* **2014**, *7*, 1131–1139.
31. Ajitha, B.; Kumar Reddy, Y.A.; Reddy, P.S.; Jeon, H.J.; Ahn, C.W. Role of capping agents in controlling silver nanoparticles size, antibacterial activity and potential application as optical hydrogen peroxide sensor. *RSC Adv.* **2016**, *6*, 36171–36179.
32. Muñoz, J.; Bastos-Arrieta, J.; Muñoz, M.; Muraviev, D.; Céspedes, F.; Baeza, M. CdS quantum dots as a scattering nanomaterial of carbon nanotubes in polymeric nanocomposite sensors for microelectrode array behavior. *J. Mater. Sci.* **2016**, *51*, 1610–1619.
33. Miller, J.N.; Miller, J.C. *Statistics of repeated measurements, in: Statistics and chemometrics for analytical chemistry*; Weston, W., Ed.; 6th ed.; Pearson: Edinburgh, UK, 2010; ISBN 9780273730422.
34. Bastos-Arrieta, J.; Muñoz, J.; Stenbock-Fermor, A.; Muñoz, M.; Muraviev, D.N.; Céspedes, F.; Tsarkova, L.A.; Baeza, M. Intermatrix Synthesis as a rapid, inexpensive and reproducible methodology for the in situ functionalization of nanostructured surfaces with quantum dots. *Appl. Surf. Sci.* **2016**, *368*, 417–426.